

# Differential Conductance and Quantum Interference in Kondo Systems

Jeremy Figgins and Dirk K. Morr

*Department of Physics, University of Illinois at Chicago, Chicago, IL 60607, USA*

(Dated: April 1, 2024)

We present a large- $N$  theory for the differential conductance,  $dI/dV$ , in Kondo systems measured via scanning tunneling spectroscopy. We demonstrate that quantum interference between tunneling processes into the conduction band and into the magnetic  $f$ -electron states is crucial in determining the experimental *Fano* lineshape of  $dI/dV$ . This allows one to uniquely extract the Kondo coupling and the ratio of the tunneling amplitudes from the experimental  $dI/dV$  curve. Finally, we show that  $dI/dV$  directly reflects the strength of the antiferromagnetic interaction in Kondo lattice systems.

PACS numbers: 75.20.Hr, 74.55.+v, 71.27.+a, 72.15.Qm

Recent progress in scanning tunneling spectroscopy (STS) techniques have made it possible for the first time to measure the differential conductance,  $dI/dV$ , in heavy-fermion compounds [1]. These materials, whose essential ingredients are a (Kondo) lattice of magnetic moments that is coupled to a conduction band [2], exhibits a variety of puzzling phenomena, ranging from non-Fermi-liquid behavior to unconventional superconductivity [3]. Their microscopic origin likely lies in the competition between an antiferromagnetic ordering of the magnetic moments, and their screening by conduction electrons [2], though no theoretical consensus has emerged as yet [4]. STS experiments, by providing insight into the local electronic structure [1] of heavy-fermion materials, might hold the key to understanding their complex properties. The theoretical challenge in the interpretation of the differential conductance in Kondo lattice systems [5], and around single Kondo impurities [6–10] arises from the quantum interference between electrons tunneling into the conduction band and into the magnetic  $f$ -electron states. While  $dI/dV$  for a single Kondo impurity has been successfully described [6–9] using a phenomenological form derived by Fano [11], a microscopic understanding of how the interplay between the strength of the Kondo coupling, the interaction between the magnetic moments, the electronic structure of the screening conduction band, and quantum interference determines the  $dI/dV$  lineshape, is still lacking.

In this Letter, we address this issue within the framework of a large- $N$  theory and identify the microscopic origin for the form of the differential conductance not only around single Kondo impurities but also in Kondo lattice systems. In particular, we demonstrate that the lineshape as well as the spatial dependence of  $dI/dV$  sensitively depend on the particle-hole asymmetry of the (screening) conduction band, as well as the quantum interference between the two tunneling paths. For a single Kondo impurity, this sensitivity allows one to uniquely extract the Kondo coupling,  $J$ , as well as ratio of the tunneling amplitudes into the conduction band and magnetic  $f$ -electron states,  $t_c$  and  $t_f$ , respectively, from the experimental STS data. In addition, for a Kondo lattice,

the  $dI/dV$  lineshape provides insight into the strength of the interaction between the magnetic moments. Due to quantum interference effects, which can lead to a reversal in the asymmetry of the  $dI/dV$  lineshape already for small changes in  $t_f/t_c$ , the differential conductance is in general qualitatively different from the local density of states (LDOS) of either the conduction band or the  $f$ -electron states. However, once the pertinent parameters are extracted from a theoretical fit, we can predict the frequency and spatial dependence of the LDOS for both bands, as well as the electronic correlations between them, thus providing important insight into the complex electronic structure of Kondo systems.

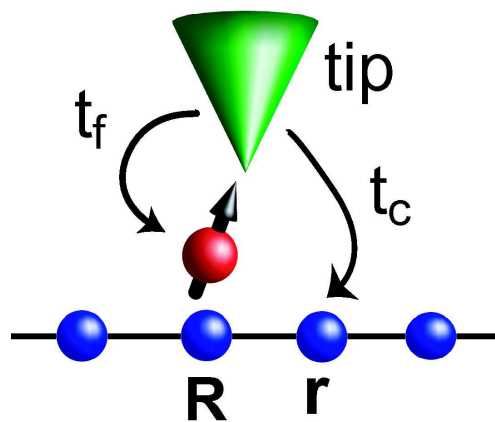


FIG. 1: (color online) Tunneling paths from the STS tip into the conduction electron and  $f$ -electron states with tunneling amplitudes  $t_c$  and  $t_f$ , respectively.

We start by considering the differential conductance in a system with a single Kondo impurity, whose Hamiltonian is given by

$$\mathcal{H} = - \sum_{\mathbf{r}, \mathbf{r}', \sigma} t_{\mathbf{r}\mathbf{r}'} c_{\mathbf{r}, \sigma}^\dagger c_{\mathbf{r}', \sigma} + J \mathbf{S}_{\mathbf{R}}^K \cdot \mathbf{s}_{\mathbf{R}}^c, \quad (1)$$

where  $t_{\mathbf{r}\mathbf{r}'}$  is the fermionic hopping element between sites  $\mathbf{r}$  and  $\mathbf{r}'$  of the conduction band,  $c_{\mathbf{r}, \sigma}^\dagger$  ( $c_{\mathbf{r}, \sigma}$ ) creates (annihilates) a fermion with spin  $\sigma$  at site  $\mathbf{r}$ , and the sums

run over all sites of the conduction band.  $\mathbf{S}_{\mathbf{R}}^K$  and  $\mathbf{s}_{\mathbf{R}}^c$  are the spin operators of the Kondo impurity and the conduction electrons at site  $\mathbf{R}$ , respectively, and  $J > 0$  is the Kondo coupling. To describe the Kondo screening of the magnetic impurity, we employ a *large- $N$*  expansion [12–18] in which  $\mathbf{S}_{\mathbf{R}}^K$  is generalized to  $SU(N)$  and represented via Abrikosov pseudofermions  $f_m^\dagger, f_m$ . These obey the constraint  $\sum_{m=1\dots N} f_m^\dagger f_m = 1$  where  $N = 2S + 1$  is the spin degeneracy of the magnetic impurity. This constraint is enforced by means of a Lagrange multiplier  $\varepsilon_f$ , while the exchange interaction in Eq.(1) is decoupled via a hybridization field,  $s$ . On the saddle point level,  $\varepsilon_f$  and  $s^2$  are obtained by minimizing the effective action [13]. Finally, the tunneling process into a conduction electron state at  $\mathbf{r}$  and the  $f$ -electron state at  $\mathbf{R}$ , as schematically shown in Fig. 1, is described by

$$\mathcal{H}_T = \sum_{\sigma} t_c c_{\mathbf{r},\sigma}^\dagger d_{\sigma} + t_f f_{\mathbf{R},\sigma}^\dagger d_{\sigma} + H.c. , \quad (2)$$

where  $d_{\sigma}$  destroys a fermion in the STS tip. The total current flowing from the tip into the systems is [19]

$$I(V) = -\frac{e}{\hbar} \text{Re} \int_0^V \frac{d\omega}{2\pi} \left[ t_c \hat{G}_{12}^K(\omega) + t_f \hat{G}_{13}^K(\omega) \right]. \quad (3)$$

Here

$$\hat{G}^K(\omega) = [\hat{1} - \hat{g}^r(\omega)\hat{t}]^{-1} \hat{f}_0(\omega) [\hat{1} - \hat{t}\hat{g}^a(\omega)]^{-1} \quad (4)$$

is the full Keldysh Greens function matrix,  $\hat{t}$  is the symmetric hopping matrix with  $\hat{t}_{12} = t_c$ ,  $\hat{t}_{13} = t_f$ , and zero otherwise.  $\hat{g}^r(\omega)$  and  $\hat{f}_0(\omega)$  are the retarded and Keldysh Greens function matrices of the Kondo system with

$$\begin{aligned} \hat{f}_0(\omega) &= 2i(1 - 2\hat{n}_F(\omega)) \text{Im}[\hat{g}^r(\omega)] ; \\ \hat{g}^r(\omega) &= \begin{pmatrix} g_t^r(\omega) & 0 & 0 \\ 0 & g_{cc}^r(\mathbf{r}, \mathbf{r}, \omega) & g_{cf}^r(\mathbf{r}, \mathbf{R}, \omega) \\ 0 & g_{fc}^r(\mathbf{R}, \mathbf{r}, \omega) & g_{ff}^r(\mathbf{R}, \mathbf{R}, \omega) \end{pmatrix} , \end{aligned} \quad (5)$$

where  $g_t^r, g_{cc}^r$  and  $g_{ff}^r$  are the local Greens functions of the tip, conduction and  $f$ -electron states, respectively, and  $g_{fc}(\mathbf{R}, \mathbf{r}, \tau) = -\langle T_{\tau} f_{\mathbf{R}}^\dagger(\tau) c_{\mathbf{r}}(0) \rangle$ . Moreover,

$$\hat{n}_F(\omega) = \begin{pmatrix} n_F^t(\omega) & 0 & 0 \\ 0 & n_F(\omega) & 0 \\ 0 & 0 & n_F(\omega) \end{pmatrix} \quad (6)$$

with  $n_F^t$  ( $n_F$ ) being the Fermi-distribution function of the tip ( $f$ - and  $c$ -electron states). While the results shown below are obtained from Eq.(3) via differentiation, it is instructive to consider the leading order contributions to  $dI/dV$  in the weak-tunneling limit,  $t_c, t_f \rightarrow 0$ , given by

$$\begin{aligned} \frac{dI(V)}{dV} &= \frac{2\pi e}{\hbar} N_t [t_c^2 N_c(\mathbf{r}, V) + t_f^2 N_f(\mathbf{R}, V) \\ &\quad + 2t_c t_f N_{cf}(\mathbf{r}, \mathbf{R}, V)] \end{aligned} \quad (7)$$

with  $N_t, N_c$  and  $N_f$  being the density of states of the tip, conduction and  $f$ -electron states, respectively, and  $N_{cf} = -\text{Im}g_{cf}^r/\pi$ . The last term in Eq.(7) describes quantum interference processes between the two tunneling paths, which, as we show below, are crucial in determining the lineshape of the differential conductance.

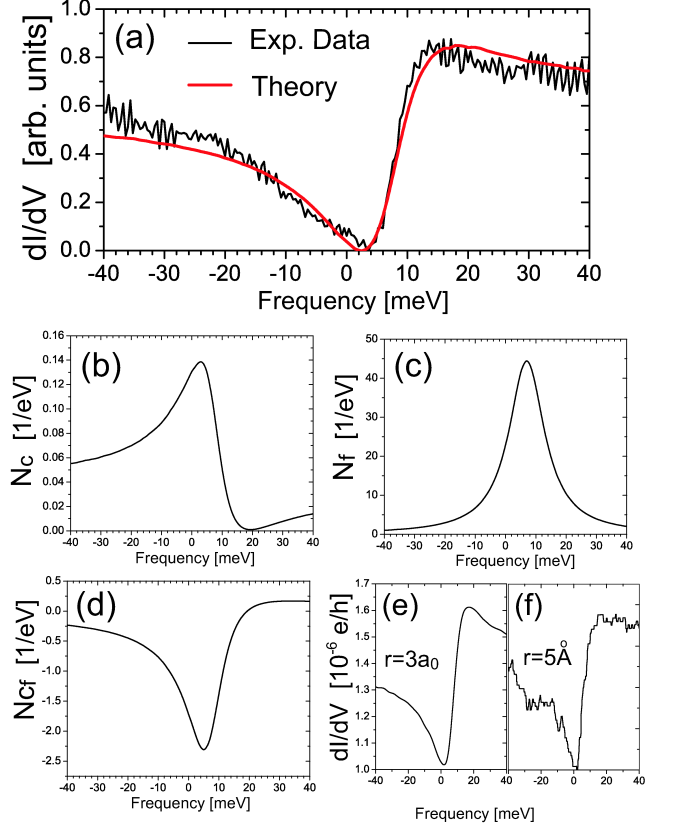


FIG. 2: (color online) (a) Experimental  $dI/dV$  curve of Ref. [9] at the site of a Co atom on a Au(111) surface together with a theoretical fit from Eq.(3) with  $N = 4$ ,  $t_f/t_c = 0.066$ ,  $t_c = 1$  meV,  $J = 1.39$  eV,  $s = 250$  meV,  $\varepsilon_f = 19$  meV and  $N_t = 1/eV$ . A constant background was subtracted from the experimental data. (b) conduction electron LDOS,  $N_c(\omega)$  (c)  $f$ -electron LDOS  $N_f(\omega)$ , and (d)  $N_{cf}(\omega)$  at  $\mathbf{R}$ . (e)  $dI/dV$  at a distance of  $r = 3a_0$  from the Co atom for  $t_f = 0$ . Parameters in (b)-(e) are the same as in (a). (f) Experimental  $dI/dV$  curve of Ref. [6] at  $r = 5\text{\AA}$  from the Co atom.

In Fig. 2(a) we present the experimental  $dI/dV$  data of Ref. [9] for a tip positioned above a Co atom on a Au(111) surface together with a theoretical fit obtained from Eq.(3). Here, tunneling into the conduction band involves only the state at  $\mathbf{R}$ , i.e.,  $\mathbf{r} = \mathbf{R}$ . The peak and dip in  $dI/dV$  are a direct signature of the hybridization between the conduction band and the  $f$ -electron state of the Kondo impurity and are commonly referred to as the Kondo resonance. As input parameters, we took the screening conduction band to be given by the Au(111) surface states possessing a triangular lattice structure with  $t = 1.3$  eV and  $\mu = -7.34$  eV [20], and used  $N = 4$

to describe the  $S = 3/2$  Co spin. The theoretical  $dI/dV$  curve is then solely determined by  $J$  and  $t_f/t_c$ , which control the width of the dip and the overall asymmetry of  $dI/dV$ , respectively. By performing an extensive survey, we found that there exists a unique set of parameters,  $J = 1.39$  eV and  $t_f/t_c = 0.0066$ , that yield the good quantitative agreement between the theoretical and experimental data shown in Fig. 2(a). We note that while the STS tip is positioned above the Co atom,  $t_f/t_c$  is small, likely reflecting the suppression of the tunneling process into the  $f$ -electron state by Coulomb effects. Moreover, once  $J$  is obtained from the fit, we can compute the LDOS of the conduction and  $f$ -electron states, which are presented in Figs. 2(b) and (c), respectively, as well as the electronic correlations between the two bands, as reflected by  $N_{cf}$  shown in Fig. 2(d). The lineshape of either LDOS (or of their superposition) is qualitatively different from that of  $dI/dV$ , demonstrating the importance of quantum interference in determining the latter. Finally, as the STS tip is moved away from the Co atom, direct tunneling into the  $f$ -electron state becomes suppressed and  $t_f \rightarrow 0$ . Therefore, in Fig. 2(e), we present the theoretical  $dI/dV$  curve with  $t_f = 0$  at a distance of  $r = 3a_0$  from the Co atom. We note that while  $t_f = 0$  the asymmetry of  $dI/dV$  is now the same as that at the site of the Co atom, and qualitatively agrees with the experimental  $dI/dV$  curve at  $r = 5\text{\AA}$  [6] shown in Fig. 2(f), demonstrating the consistency of our approach. A more quantitative fit would require an extensive spatial survey of  $dI/dV$  away from the Co atom.

The asymmetry of the  $dI/dV$  lineshape is determined by two microscopic properties: the particle-hole asymmetry of the screening conduction band, and the ratio of the tunneling amplitudes,  $t_f/t_c$ . To demonstrate this dependence, we present in Fig. 3 the evolution of  $dI/dV$  with increasing ratio  $t_f/t_c$ . To contrast and complement the results shown in Fig. 2, we take  $N = 2$ , corresponding to a spin-1/2 moment, and consider a conduction band on a square lattice with  $t = 0.5E_0$  and  $\mu = -1.809E_0$ . The resulting circular Fermi surface with Fermi wavelength  $\lambda_F = 10a_0$  is representative of the Au(111) and Cu(111) surfaces states employed in Refs.[6, 9, 10]. For  $t_f = 0$  [solid line in Fig. 3(a)],  $dI/dV$  exhibits a Kondo resonance whose asymmetry is opposite to the experimentally observed one shown in Fig. 1(a). The asymmetry of  $dI/dV$  for  $t_f = 0$  is a direct consequence of the particle-hole asymmetry of the conduction band. Indeed, reversing the latter via  $\mu \rightarrow -\mu$ , also leads to a reversal of the asymmetry in  $dI/dV$ , as shown by the dashed line in Fig. 3(a). Moreover, with increasing  $t_f/t_c$ , the height of the peak on the negative energy side, as well as the width of the dip in  $dI/dV$  decrease while its minimum shifts to lower energies [see Fig. 3(b)], leading to an almost symmetric  $dI/dV$  curve for  $t_f/t_c = 0.062$  [see Fig. 3(c)]. Increasing  $t_f/t_c$  even further [see Fig. 3(d)] now reverses the asymmetry in  $dI/dV$ , yielding a peak on

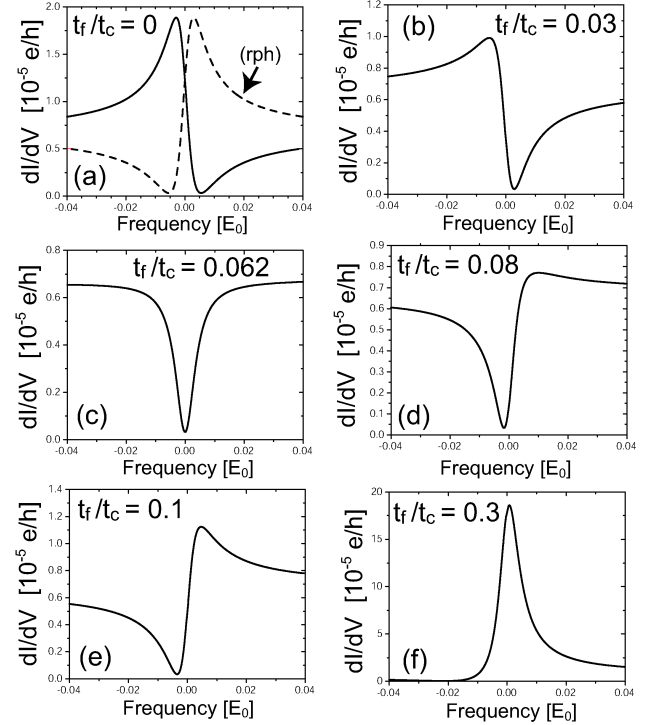


FIG. 3: (a) - (f)  $dI/dV$  at  $\mathbf{r} = \mathbf{R}$  as a function of energy for  $N = 2$ ,  $J = 0.5E_0$ ,  $N_t = 1.0/E_0$ ,  $t_c = 0.001E_0$ ,  $\varepsilon_f = 0.00520E_0$ ,  $s = 0.0847E_0$  and different values of  $t_f/t_c$ . Dashed line in (a) represents  $dI/dV$  for a conduction band with a reversed particle-hole (rph) asymmetry.

the positive energy side, and a minimum at slightly negative energies. The asymmetry of the  $dI/dV$  lineshape is now similar to that observed experimentally. However, in contrast to the case of a spin-3/2 moment ( $N = 4$ ) considered in Fig. 2(a), the minimum in  $dI/dV$  is located at negative energies for a spin-1/2 moment ( $N = 2$ ). Indeed, for  $N = 2$ , no fit to the experimental data of Fig. 2(a) can be obtained. This demonstrates that the differential conductance directly reflects the spin of the screened magnetic moment. Increasing  $t_f/t_c$  even further [see Fig. 3(f)] leads to an increase in the height of the peak and a widening of the dip.

We next turn to the discussion of the differential conductance in a Kondo lattice system, whose complex properties are determined by the competition between the Kondo screening of the magnetic moments and their antiferromagnetic ordering [2]. Its Hamiltonian is obtained by appropriately extending Eq.(1), and adding the term  $\mathcal{H}_I = \sum_{\mathbf{r},\mathbf{r}'} I_{\mathbf{r},\mathbf{r}'} \mathbf{S}_{\mathbf{r}}^K \mathbf{S}_{\mathbf{r}'}^K$  representing the antiferromagnetic interaction between the moments. Here, we take  $I_{\mathbf{r},\mathbf{r}'} > 0$  to be non-zero for nearest-neighbor sites only. Using again an Abrikosov pseudo-fermion representation of  $\mathbf{S}_{\mathbf{r}}^K$ , the Hamiltonian is decoupled by introducing the spatially uniform mean-fields [17]  $s = J \langle f_{\mathbf{r},\alpha}^\dagger c_{\mathbf{r},\alpha} \rangle$  and  $\chi_0 = I \langle f_{\mathbf{r},\alpha}^\dagger f_{\mathbf{r}',\alpha} \rangle$ , where the latter is a measure

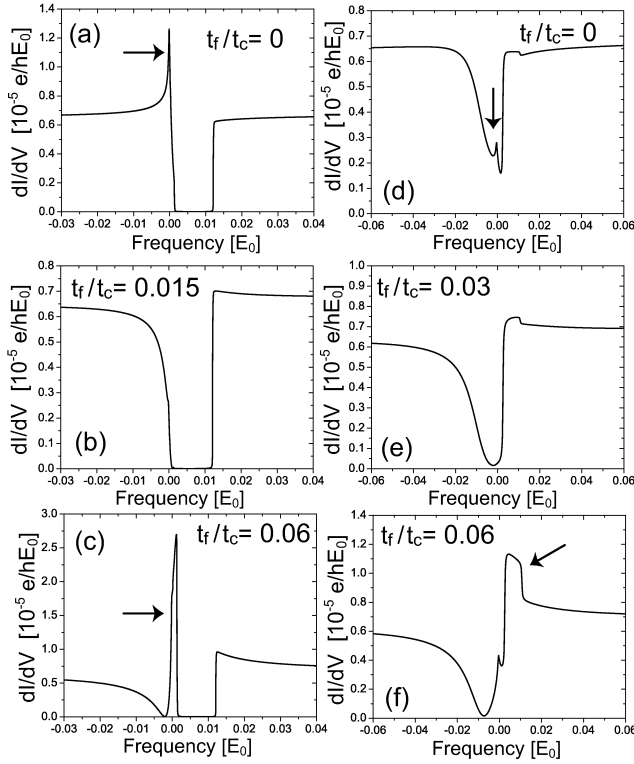


FIG. 4: Evolution of  $dI/dV$  in a Kondo lattice with  $t_f/t_c$  for  $N = 2$ ,  $J = 0.5E_0$ ,  $N_t = 1/E_0$ ,  $t_c = 0.001E_0$ , and (a) - (c)  $I/J = 0.001$  with  $\varepsilon_f = 0.0012E_0$ ,  $s = 0.0485E_0$ ,  $\chi_0 = 0.00017E_0$ , and (d) - (f)  $I/J = 0.015$  with  $\varepsilon_f = 0.00094E_0$ ,  $s = 0.0480E_0$  and  $\chi_0 = 0.00259E_0$ .

of the magnetic correlations in the system. The constraint  $\langle n_f \rangle = 1$  is enforced via a local on-site energy,  $\sum_{\mathbf{r}} \varepsilon_f f_{\mathbf{r},\alpha}^\dagger f_{\mathbf{r},\alpha}$ .

The magnetic interactions in the (screened) Kondo lattice have a profound effect on the form of the differential conductance, as shown in Fig. 4 where we present the evolution of  $dI/dV$  with  $t_f/t_c$  for two different magnetic interaction strengths,  $I/J = 0.001$  (left column) and  $I/J = 0.015$  (right column). While for  $I/J = 0.001$ ,  $dI/dV$  exhibits a hard *hybridization gap* for all values of  $t_f/t_c$ , only a suppression of the differential conductance around the Fermi energy is found for  $I/J = 0.015$ . However, in both cases,  $dI/dV$  exhibits a peak on the negative energy side (indicated by arrows), which arises from the Van Hove singularity of the large (hybridized) Fermi surface. This peak is first suppressed with increasing  $t_f/t_c$  [see Figs. 4(b) and (e)], but then reemerges together with a second peak [indicated by arrows in Figs. 4(c) and (f)], which is the precursor of the emerging *f*-electron band. This second peak is centered around the Fermi energy for  $I/J = 0.001$ , but is located at positive energies for  $I/J = 0.015$ . In the latter case, we also find a shift of the minimum in  $dI/dV$  to lower energies with increasing  $t_f/t_c$ . This qualitative difference in the differential conductance thus provides direct insight into the strength of

the antiferromagnetic interactions.

In summary, we have presented a large- $N$  theory for the differential conductance in Kondo systems. We demonstrated that quantum interference between tunneling paths is crucial in explaining the experimentally observed *Fano* lineshape of  $dI/dV$ . This allows one to uniquely extract the Kondo coupling as well as the ratio of the tunneling amplitudes from the experimental  $dI/dV$  curve. Finally, we showed that  $dI/dV$  reflects the strength of the antiferromagnetic interaction in Kondo lattice systems.

We would like to thank J.C. Davis, V. Madhavan, and H. Manoharan for stimulating discussions, and V. Madhavan for providing the data of Ref. [9]. D.K.M. would like to thank the James Franck Institute at the University of Chicago for its hospitality during various stages of this project. This work is supported by the U.S. Department of Energy under Award No. DE-FG02-05ER46225.

- 
- [1] A.R. Schmidt, M.H. Hamidian, P. Wahl, F. Meier, A.V. Balatsky, T.J. Williams, G.M. Luke and J.C. Davis, preprint, submitted.
  - [2] S. Doniach, *Physica B* **91**, 231 (1977).
  - [3] M.B. Maple *et al.*, *J. Low Temp. Phys.* **99**, 223 (1995); A. Schroder *et al.* *Nature* (London) **407**, 351 (2000); G.R. Stewart, *Rev. Mod. Phys.* **73**, 797 (2001); J. Custers, *et al.* *Nature* (London) **424**, 524 (2003); H. von Lohneysen *et al.*, *Rev. Mod. Phys.* **79**, 1015 (2007); P. Gegenwart, Q. Si, and F. Steglich, *Nature Physics*, **4**, 186 (2008).
  - [4] P. Coleman, *et al.*, *J. Phys. Cond. Mat.* **13**, R723 (2001); Q.M. Si, *et al.*, *Nature* (London) **413**, 804 (2001); P. Sun, and G. Kotliar, *Phys. Rev. Lett.* **91**, 037209 (2003); T. Senthil, S. Sachdev, and M. Vojta, *Phys. Rev. Lett.* **90**, 216403 (2003); I. Paul, C. Pepin, and M.R. Norman, *Phys. Rev. Lett.* **98**, 026402 (2007).
  - [5] M. Maltseva, M. Dzero, and P. Coleman, *Phys. Rev. Lett.* **103**, 206402 (2009).
  - [6] V. Madhavan *et al.*, *Science* **280**, 567 (1998).
  - [7] J. Li, *et al.*, *Phys. Rev. Lett.* **80**, 2893 (1998).
  - [8] O. Ujsaghy *et al.*, *Phys. Rev. Lett.* **85**, 2557 (2000).
  - [9] V. Madhavan, *et al.*, *Phys. Rev. B* **64**, 165412 (2001).
  - [10] H.C. Manoharan, C.P. Lutz, and D.M. Eigler, *Nature* (London) **403**, 512 (2000).
  - [11] U. Fano, *Phys. Rev.* **124**, 1866 (1961).
  - [12] B. Coqblin and J.R. Schrieffer, *Phys. Rev.* **185**, 847 (1969).
  - [13] N. Read and D. M. Newns, *J. Phys. C* **16**, 3273 (1983).
  - [14] P. Coleman, *Phys. Rev. B* **28**, 5255 (1983).
  - [15] A.J. Millis and P.A. Lee, *Phys. Rev. B* **35**, 3394 (1987).
  - [16] N. E. Bickers, *Rev. Mod. Phys.* **59**, 845 (1987).
  - [17] T. Senthil, S. Sachdev, and M. Vojta, *Phys. Rev. B* **69**, 035111 (2004).
  - [18] E. Rossi and D.K. Morr, *Phys. Rev. Lett.* **97**, 236602 (2006).
  - [19] K. Caroli *et al.*, *J. Phys. C: Solid St. Phys.* **4**, 916 (1971).
  - [20] C. Schouteden, P. Lievens, and C. Van Haesendonck, *Phys. Rev. B* **79**, 195409 (2009).